10.5005/jp-journals-10003-1073

INVITED ARTICLE

Imaging in Common Anterior and Sellar/ Perisellar Skull Base Lesions

Zena M Patel, Santosh S Gupta

Consultant Radiologists, Department of Imaging, PD Hinduja National Hospital and Medical Research Centre, Mumbai, Maharashtra, India

Correspondence: Zena M Patel, Consultant Radiologists, Department of Imaging, PD Hinduja National Hospital and Medical Research Centre, Veer Savakar Marg, Mumbai-400016, Maharashtra, India, e-mail: patelzena@hotmail.com

ABSTRACT

Skull base surgery is an advanced surgical subspeciality. A wide range of pathologies can primarily or secondarily involve the skull base. Due to its complex anatomy, cross-sectional imaging is an important part in the multidisciplinary approach for skull base lesions.

Keywords: Anterior, Skull base, Imaging.

INTRODUCTION

The skull base separates the brain and meninges from the neck-face region. Multiple foramina through which neurovascular structures course. Imaging helps in diagnosing the various lesions which involve the skull base on the basis of their typical sites and morphology. In case of neoplasms imaging is useful in staging them, determining the extent of involvement, surgical feasibility, approach and postoperative recurrence. CT and MRI play a complementary role in preoperative evaluation of skull base lesions. CT provides a roadmap of the bony anatomical landmarks, which are used to identify the site of important neurovascular structures during surgery. MR helps in identifying the type of lesion, its vascularity, its relation with vessels, nerves and involvement/encasement of the adjacent neurovascular structures, dura and bone marrow. CT and MR are also performed prior to the CSF repair surgery to identify the exact site of leak. This article focuses on the basic anatomy, and common pathologies which involve the anterior skull base and sellar/perisellar regions.

Imaging Techniques

CT and MRI are now widely available and are the modalities of choice for skull base imaging.

CT

CT is very useful in depicting the bony anatomy. It can differentiate between various types of osseous involvement, such as destruction, erosion, scalloping, remodeling, expansion, sclerosis, which are often a clue to the diagnosis. For example, smooth bony margin favors a benign pathology like schwannoma, whereas destruction is suggestive of an aggressive etiology. Reactive sclerosis is seen with meningiomas and chronic sinus infection. Tumor matrix is best characterized on CT, for example in chondrosarcoma, ring and arc calcification is seen within the lesion. Foraminal widening, associated with perineural spread is also better seen on CT. CT is the modality of choice for diagnosing fibro-osseous dysplasias. At our center we tailor the study depending on the indication. Routinely for skull base lesions a limited axial plain study is done followed by axial post-intravenous contrast scan. Thin 0.6 mm sections are obtained which are later reformatted into 3 mm thick sagittal and coronal planes. Images are reviewed in both bone and soft tissue windows setting (2000/500 and 300/50 respectively). Occasionally skull base lesions are incidentally seen on the limited plain sequential coronal paranasal sinus CT study. In these cases the study is completed with a post-contrast axial helical study. In patients with a suspected CSF leak, we perform a plain high resolution 0.6 mm oblique coronal CT, followed by a post intrathecal contrast study (discussed in detail under the heading of CT cisternography).

MRI

Combination of various pulse sequences and multiplanar capability makes MRI more superior for evaluation of the skull base. It should be used as the primary imaging modality of choice in most cases and may be complemented with a CT whenever required. Various pulse sequences are available, which help in differentiating the lesion on basis of the soft tissue signal characteristics. Subtle bone marrow involvement (when no erosion is seen on CT) can be seen on MRI. High resolution, thin (3-4 mm slice thickness) and small FOV is used to obtain the various sequences. The skull base imaging protocol includes precontrast axial and coronal T1-weighted and T2-weighted sequences, with T2-weighted fat saturation in any one plane. Postcontrast axial and coronal T1-weighted fat saturated sequences are performed. Dedicated thin sagittal sequences are performed for sellar and other midline lesions, e.g. congenital midline nasofrontal masses. Limited sequences for whole brain are

also performed. Fatty marrow appears bright on T1-weighted images. Direct tumor involving bone appears hypo- to isointense and is well-appreciated on these sequences. Postcontrast axial and coronal fat saturated sequences; maximize the contrast between the enhancing lesion and the marrow which appears dark due to fat suppression. The enhancement is subjectively graded as mild, moderate or intense. Also noted is whether there is homogeneous or heterogeneous enhancement. Postcontrast sequences are very sensitive to look for perineural spread and dural involvement. Axial and coronal T2-weighted sequences are performed, one of which is with fat saturation. The soft tissue chararacteristics of the lesion are demonstrated on these sequences. They are described as iso, hypo or hyperintense and homogeneous or heterogeneous. T2 dark areas may sometimes represent blood or calcium. Other etiologies like fungal infections, inflammatory pseudotumors, tuberculosis and meningiomas can be T2 hypointense. Dedicated sagittal planes are perfomed in case of midline/paramedian lesions, e.g. congenital midline nasofrontal anomalies, anterior skull base meningiomas, sellar-parasellar lesions, clival tumors, etc. In case of suspected infections, diffusion weighted axial sequence can be done to look for abscess formation. FIESTA (fast imaging employing steady state acquisition) is a fast steady state free precession gradient echo sequence with a short acquisition time. There is good background signal suppression with the fluid filled structures appearing very bright. This sequence is useful for evaluation of CSF leaks, to visualize cranial nerves and congenital skull base anomalies.

Other Imaging Modalities

DSA is not routinely performed in patients with a skull base pathology. However, in case of juvenile nasal angiofibroma, preoperative catheter angiography with embolization is performed to reduce the intraoperative blood loss. DSA is also useful in diagnosing caroticocavernous fistulae and paragangliomas.

With the advent of multislice CT and MRI, plain radiographs and tomograms are not used for evaluating skull base pathology.

Relevant Anatomy (Figs 1 to 3)

The anterior skull base forms the floor of the anterior cranial fossa and the roof of the orbits laterally and paranasal sinuses and nasal cavity in the median plane. The anterior border is formed by the posterior wall of the frontal sinus. The anterior clinoid processes and planum sphenoidale form the posterior margin. The latter forms the roof of the sphenoid sinus. The lateral border is formed by the frontal bone on both sides. The cribriform plate of the ethmoid bone is a thin bone which lies centrally and forms the roof of the nasal cavity. It has a medial horizontal lamella and a lateral vertical lamella and contains multiple perforations through which the olfactory nerves traverse and enter the nasal cavity. It

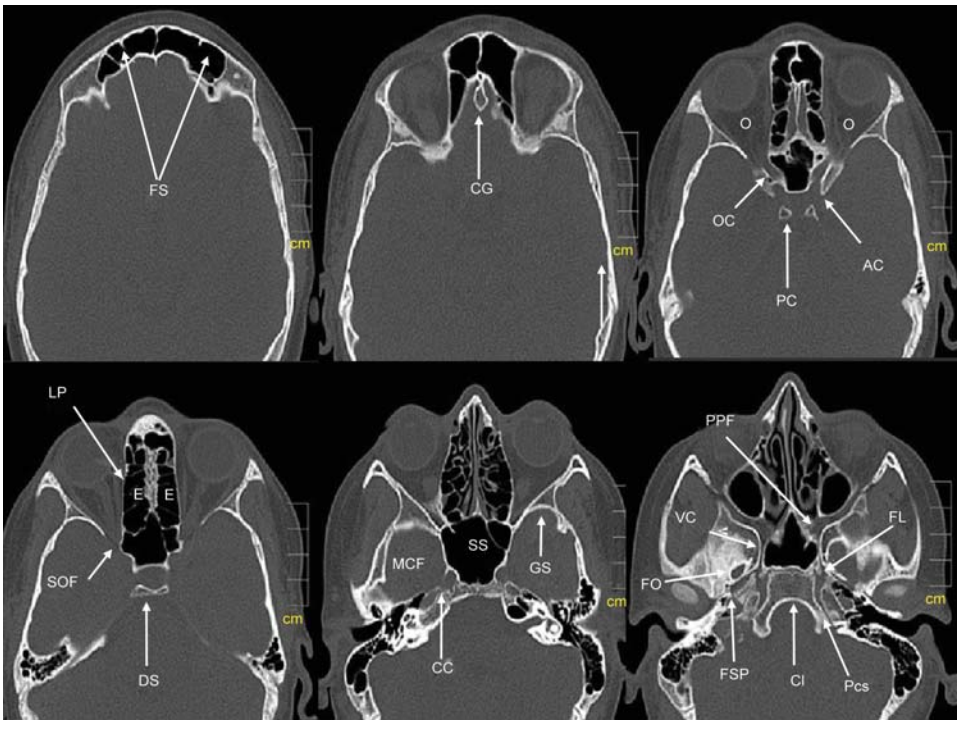

Fig. 1: Axial CT bone window, FS: Frontal sinus; CG: Crista gallioc; OC: Optic canal; AC: Anterior clinoid process; PC: Posterior clinoid process; O: Orbit; LP: Lamina paparacea; E: Ethmoid air cells; DS: Dorsum sellae; SOF: Superior orbital fissure; SS: Sphenoid sinus; GS: Greater wing of sphenoid; MCF: Middle cranial fossa; CC: Carotid canal; FO: Formane ovale; FSP: Foramen spinosum; VC: Vidian canal; FL: Foramen lacerum; PCS: Petroclival suture; Cl: Clivus; PPF: Pterygopalatine fossa

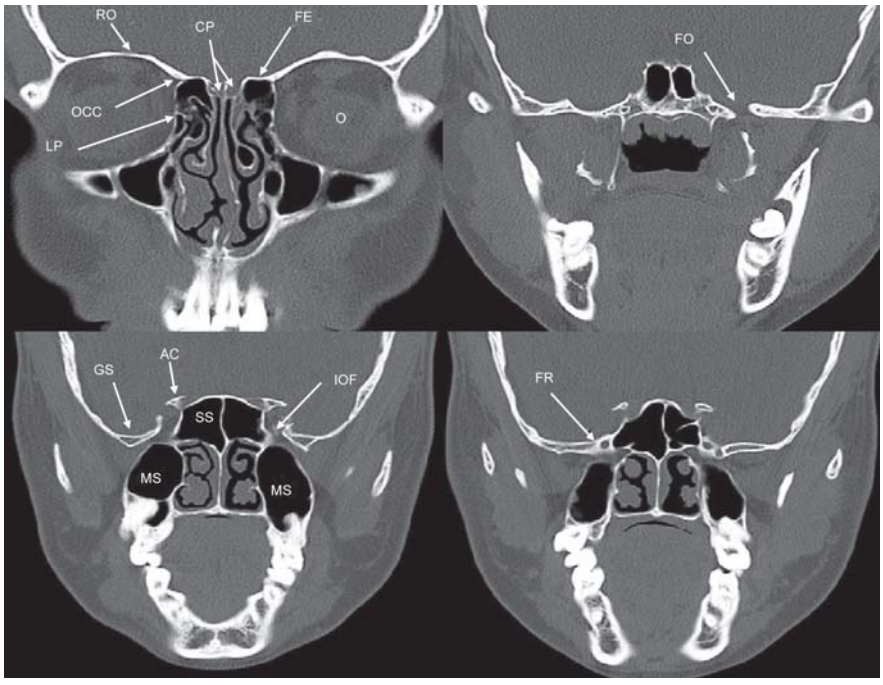

Fig. 2: Coronal CT bone window: CP: Cribriform plate; FE: Fovea ethmoidalis; RO: Roof of orbit; O: Orbit; OCC: Orbitocranial canal; LP: Lamina papracea; GS: Greater wing of sphenoid; IOF: Inferior orbital fissure; FR: Foramen rotundum; MS: Maxillary sinus; AC: Anterior clinoid process; FO: Foramen ovale

continues laterally with a thicker fovea ethmoidalis which forms the roof of the ethmoid sinus.The cribriform plate lies about 1cm lower than the fovea ethmoidalis, which is important for the surgeons to know during transethmoidal surgery. The greater part of the anterior skull base is formed by the laterally located orbital portion of the frontal bone, which forms the roof of the orbit. An important landmark for surgery is the orbitocranial canal through which the anterior ethmoid artery courses from the orbit into the ethmoid sinus and then into the anterior cranial fossa. It is a potential site of injury to the thin cribriform bone during surgery. The foramen caecum is a midline blind ending structure. Its patency leads to the formation of the various midline developmental anomalies. The crista galli is a midline vertical structure in the anterior frontal region to which the anterior falx attaches. The olfactory bulb lies along the medial margin of the orbital process of the frontal bone. Posteriorly, it continues and courses above the cribriform plate and planum sphenoidale as the olfactory tract.

The central skull base is mainly formed by the sphenoid bone. The pituitary gland is situated in the sella turcica which is a depression within the sphenoid bone. It lies postero-superior to the sphenoid sinus. Anteriorly is the planum-sphenoidale which articulates with the cribriform plate. The tuberculum sellae lies posterior to the planum. The anterior clinoid processes are situated lateral to it and abut the optic canal. The dorsum sella is the posterior wall of the sella which terminates laterally into the posterior clinoid process. The lesser wing of the sphenoid are plate like bones which project from either side of the anterior sphenoid body. The

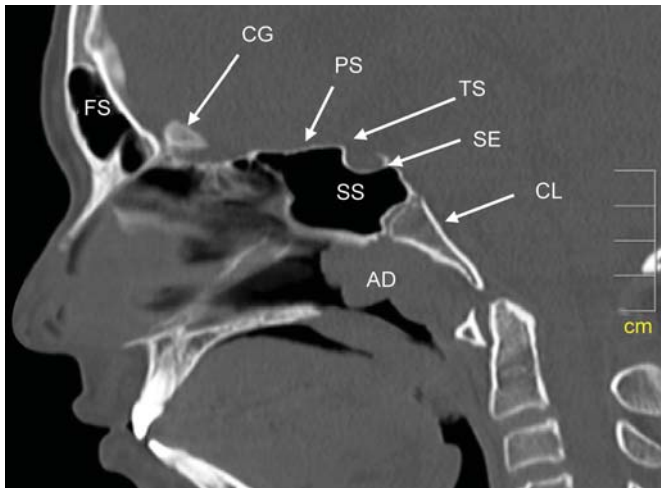

Fig. 3: Sagittal CT bone window: FS: Frontal sinus; CG: Crista galli; PS: Planum sphenoidale; TS: Tuberculum sellae; SE: Sella; Cl: Clivus; SS: Sphenoid sinus; AD: Adenoids

greater wing of the sphenoid are bow shaped bones which arise from the inferolateral aspect of the sphenoid body and course upward and laterally. They form the floor of the middle cranial fossa. The optic canal transmits the optic nerve and ophthalmic artery and lies at the apex of the orbit within the sphenoid bone. The upper margin of the superior orbital fissure is formed by the lesser wing of the sphenoid, while its inferior margin is formed by the greater wing. The inferior orbital fissure transmits the maxillary nerve (CN V2) and infraorbital vessels, and it communicates with the infratemporal and pterygomaxillary fossae. The lateral portion of the IOF is an important surgical landmark for positioning lateral orbital osteotomies during anterior skull

base resections. The medial and lateral pterygoid plates are paired bony processes, which arise from the inferior portion of the sphenoid body. The foramen ovale, spinosum and rotundum and the vidian canal, all lie within the sphenoid bone. The cavernous sinuses lie on either side of the sphenoid bone. The oculomotor (III), trochlear (IV) and the ophthalmic and maxillary divisions of the trigeminal (V) nerve traverse through the lateral wall of the sinus on both sides. The abducens (VI) nerve and cavernous segment of the internal carotid artery course through the cavernous sinus. The Meckel's cave which contains the trigeminal ganglion is seen as focal fluid density area, posteroinferior to the cavernous sinus.

The clivus is a midline bone which lies posterior to the sphenoid sinus and the nasopharynx, inferior to the sella. Laterally the petro-occipital fissure separates it from the petrous bone. Bone tumors like chordoma and chondrosarcoma arise in this region. Secondary involvement of the clivus is seen in base skull osteomyelitis, invasive pituitary adenoma, etc.

Pathology

In this article we have subdivided the common skull base pathologies into the following subgroups:

Tumors-sinonasal
- Juvenile angiofibroma
- Fibro-osseous lesions
- Squamous carcinoma
- Adenocarcinoma
- Minor salivary gland tumors
- Esthesioneuroblastoma
- Melanoma
- Lymphoma

Tumors-intracranial
- Meningioma
- Schwannoma
- Pituitary adenoma
- Craniopharyngioma
- Chondrosarcoma
- Chordoma
- Metastases

Infective/Inflammatory
- Invasive fungal sinusitis
- Mucocele
- Inflammatory pseudotumor
- Tuberculosis

CSF fistula

Congenital
- Dermoid and epidermoid
- Meningoencephalocele
- Nasal glioma

JUVENILE NASOPHARYNGEAL ANGIOFIBROMA

They are benign vascular neoplasms which occur in adolescent males. The sphenopalatine foramen is the early site of involvement, from where these tumors extend into various fissures and formanina. They can extend medially into the nasopharynx, laterally into the pterygopalatine fossa, superiorly into the middle cranial fossa through the vidian canal or foramen rotundum, through the infraorbital fissure into the infratemporal fossa and into the maxillary and ethmoid sinuses. They are highly vascular tumors and usually present

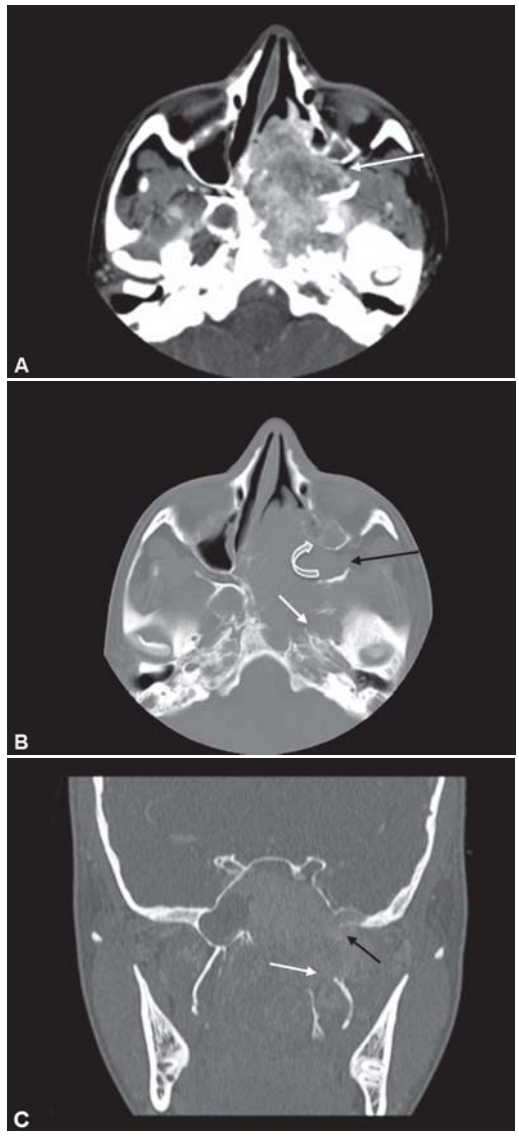

Figs 4A to C: Juvenile nasopharyngeal angiofibroma in a 15-year-old male. (A) Axial postcontrast CT scan of the neck shows a large enhancing mass lesion in the left nasal fossa extending laterally into the left sphenopalatine foramen and pterygopalatine fossa (white arrow) and posteriorly into the nasopharynx and central skull base, (B) axial CT bone window shows widening of the left pterygopalatine fossa (black arrow) and characteristic anterior displacement of the posterior wall of the left maxillary sinus (curved white arrow) with erosion of the clivus and left petrous bone (straight white arrow), (C) coronal CT bone window reveals erosion of the left pterygoid plates (white arrow), medial aspect of the left greater wing of the sphenoid (black arrow) and floor of the sphenoid sinus with extension into the sphenoid sinus

with epistaxis. Frank bone destruction is a not common feature; however, they do cause bone remodeling and erosion.[1,2] One of the classical signs is anterior bowing of the posterior wall of the maxillary sinus (Figs 4A to C) and widening of the pterygopalatine fossa and pterygomaxillary and inferior orbital fissures.[3,4] CT reveals a brilliantly enhancing unencapsulated posterior nasal or nasopharyngeal mass. CT is very useful in looking for extension into adjacent foramina and fissures, which this lesion has a high propensity to involve. Since, the recurrence rate following surgery is high, these patients are routinely followed up with imaging. The role of MRI is mainly to look for intracranial extension and to differentiate retained sinus secretions from sinus invasion.[1] On catheter angiography these lesions have an intense capillary blush along with a feeder artery. Preoperative catheter angiography embolization is often done to reduce the intraoperative blood loss.

FIBRO-OSSEOUS LESIONS

Fibrous dysplasia and osteomas are common tumors which involve the calvarium.

Fibrous dyplasia is a developmental skeletal abnormality of unknown etiology. 10 to 25% of patients of monostotic fibrous dysplasia and 50% of patients with polyostotic fibrous dysplasia have involvement of the skull and facial bones.[5] There are three patterns seen on CT: The ground-glass pattern (56%), the homogeneously dense pattern (23%), and the cystic variety (21%).[6] An expanded bone with a ground glass matrix is a characteristic finding of fibrous dyplasia on CT. On MR the localized form can be mistaken for tumors, hence knowledge of the potential diagnostic pitfall can help prevent surgery for these lesions. The T1 appearance varies depending on the ratio of fibrous tissue to mineralized matrix. Lesions with high fibrous tissue content appear intermediate on T1-weighted images. The MR appearance on T2-weighted images is variable. Few lesions with a highly mineralized matrix appear hypointense, whereas nonmineralized and cystic areas appear hyperintense on T2-weighted images. The nonmineralized areas contain metabolically active fibrous tissue, which appears T2 hyperintense.[7] Intense postcontrast enhancement is seen due to the highly vascular nature of these lesions.[8] Frank destruction and associated soft tissue is not a feature of fibrous dysplasia.

OSTEOMAS

They are benign fibro-osseous lesions which usually involve the membranous bones of the skull and face, the frontal and ethmoid sinuses being the common sites. They can present with a forehead swelling or symptoms of sinus disease and headache. They are of two types: Ivory-type which appear as densely sclerotic lesions on CT and hypointense on both T1 and T2-weighted images on MR. The other type is the fibrous osteoma, which is less ossified.[9] They appears inhomogeneous with an intermediate to low signal intensity on all MR sequences.

SQUAMOUS CARCINOMA

Squamous all carcinoma is the most common sinonasal malignancy and accounts for 80% of all paranasal sinus malignancies. The maxillary antrum is the most common site.[1,10] The nasal cavity and ethmoid sinuses are the other sites. Frontal and sphenoid sinuses are rarely involved.[11,12] Males are more commonly affected with the average age of presentation being 50 years.[11,13] They are aggressive tumors and cause bony destruction which is well-depicted on CT. On MRI the tumor has an intermediate signal intensity on T2-weighted images with postcontrast enhancement seen as against inspissated secretions, mucoceles and polyps which do not enhance, thus helping distinguish them from these benign conditions. Direct extension into the anterior cranial fossa through the cribriform plate is well seen on coronal postcontrast sequences. Dural enhancement and perineural spread are also better appreciated on postcontrast MRI than CT. Nasopharyngeal squamous cell carcinomas is one of the common head and neck cancers which can cause adjacent marrow changes and bony destruction. Obstruction of the eustachian tube can also be seen, wherin the patient may present with ipsilateral ear symptoms (Figs 5A and B).

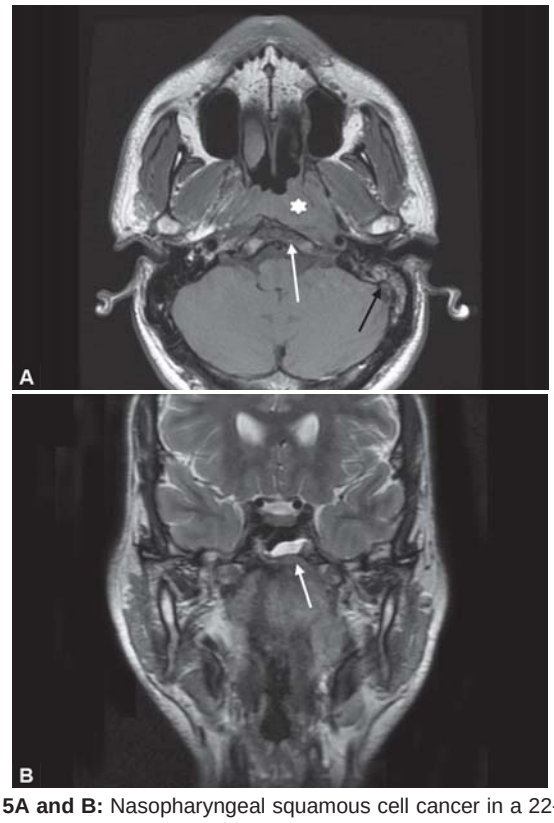

Figs 5A and B: Nasopharyngeal squamous cell cancer in a 22-year-old male: (A) Axial T1-weighted sequence shows an isointense nasopharyngeal mass on the left side (*) with focal marrow edema in the clivus (white arrow) and opacified left mastoid air cells (black arrow) due to Eustachian tube blockage, (B) coronal T2-weighted sequence a heterogeneous mass along the roof and left lateral aspect of the nasopharynx with erosion of the floor of the sphenoid sinus (white arrow)

ADENOCARCINOMA

Ten percent of all sinonasal tumors are adenocarcinoma. They are further subdivided into minor salary gland tumors, intestinal type adenocarcinoma and neuroendocrine tumors.[9] They often occur in the 6th decade with males affected more commonly. There are no specific features of adenocarcinoma on imaging which can differentiate it from squamous carcinoma.

MINOR SALIVARY GLAND TUMORS

It includes multiple pathologies, the commonest being adenoid cystic carcinoma. They are slow growing tumors; however, they cause bony destruction and have a high incidence of perineural spread. The trigeminal and facial are the most common nerves to be involved in perineural spread.[14] On MR, perineural spread is seen as abnormal enhancement and thickening of the nerve. Widening of the foramen/canal may also be seen on the bone window setting on CT. In case of the trigeminal nerve it is best seen on the postcontrast coronal fat saturated sequence. Distant metastases are common in these tumors, occurring in approximately 40% cases. Regional lymph node involvement on the other hand is rare.[11,15]

ESTHESIONEUROBLASTOMA

They are rare tumors of neural crest origin that arise from the olfactory neuroepithelium in the superior recess of the nasal cavity. A bimodal peak of incidence in the 2nd and 6th decades is observed. They are slow growing tumors and usually present with nasal obstruction, epistaxis and anosmia. On CT they are seen as solid homogeneously enhancing soft tissue lesions in the superior nasal cavity. Focal calcification is occasionally seen, which can aid in the diagnosis.[16] Owing to their slow growth, bone remodeling and resorption are seen more often than frank bony destruction. Intracranial extension is seen in 25% of cases.[17] These lesions are of variable T1-weighted and T2-weighted signal with some heterogeneity and minimal to moderate gadolinium enhancement (Figs 6A to C). Peripheral tumoral cysts can be seen in the intracranial component and are quite characteristic of this tumor.[18] Coronal MR sequences are useful in looking for meningeal and intracranial involvement.

MELANOMAS

Melanomas of the nasal cavity and paranasal sinuses arise from the melanocytes that have migrated during embryologic development from the neural crest to the sinonasal mucosa.[11,19] The nasal cavity is the most common location of melanoma in the head and neck region. Sinonasal melanomas often arise from the turbinates on the nasal septum.[11,20] The MRI appearance of a melanotic melanoma is very typical, appearing bright on the precontrast T1-weighted images. It can cause remodeling of the bone which can falsely favor a benign pathology. Frank bony erosion also can be present. Following contrast administration, melanomas enhance avidly.

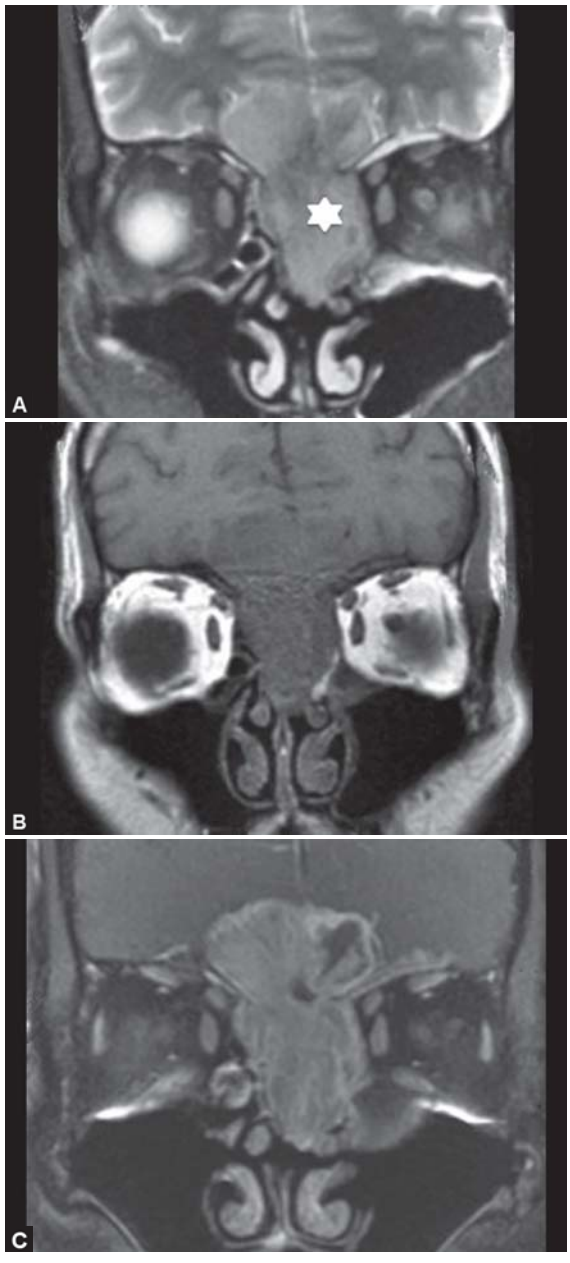

Figs 6A to C: Esthesioneuroblastoma: (A) Coronal T2-weighted image shows a heterogeneous intermediate signal intensity mass lesion in the midline nasal cavity and ethmoid (*), with intracranial extension, (B) coronal T1-weighted image shows hypointense signal in this mass, (C) coronal postcontrast T1-weighted fat suppressed image shows heterogeneous enhancement in this mass, with the intracranial extension better appreciated

SINONASAL LYMPHOMA

Lethal midline granuloma is another name for it. 44% of extranodal lymphomas arise in the sinonasal region. It is a T cell lymphoma and is associated with Ebstein-Barr virus.[11]

In the initial stages it is seen as nodular mucosal thickening. Wagener's granulomatosis and cocaine abuse are the differentials. As it grows it causes slow and progressive destruction of the nasal septum and turbinates.[9,21] On T2-weighted images it appears as a bulky iso- to hypointense homogeneous mass. Homogeneous postcontrast enhancement is seen. Associated findings of bone remodeling or erosion can be present.

MENINGIOMA

They are benign tumors which arise from the rests within arachnoid villi in relation to the margin of the dural sinus. They occur at various sites in the skull base, namely the diaphragm and tuberculum sellae, anterior and posterior clinoid processes, olfactory groove, planum sphenoidale and cavernous sinus dura.[22-24] On MRI they appear as broad based extra-axial masses, hypointense on T1-weighted images and iso- to hypointense on the T2-weighted images due to high cellularity. In majority of the cases homogeneous postcontrast enhancement is seen with a linear enhancing dural tail. Hyperintense signal on diffusion weighted images can be seen due to high cellularity. Olfactory groove meningiomas may extend inferiorly into the nasal cavity and ethmoid air cells through the cribriform plate. The sellar and parasellar menigiomas account for 20 to 25% of all meningiomas.[25-28] They tend to displace the pituitary gland (Figs 7A and B). They appear hyperdense on plain CT with homogeneous postcontrast enhancement. CT also demonstrates intralesional calcification along with hyperostosis and erosions in the adjacent bones (Figs 8A and B). Sphenocavernous and petroclival meningiomas are seen in the parasellar and central skull base region. They grow on either side of the petrous bone and extend into the posterior fossa where they can compress the brainstem, basilar artery and/or its branches. Medially they can invade the sphenoid sinus and sella. Anterior extension into superior orbital fissure and orbital apex, lateral extension into the floor of middle cranial fossa and inferolateral extension into the masticator space can be seen.[29-32]

Figs 7A and B: Parasellar meningioma in a 55-year-old female: (A) Axial T2-weighted fat saturated sequence shows a left parasellar T2 dark mass lesion (*) extending into the medial temporal region and left prepontine region, (B) coronal T1-weighted fat saturated postcontrast sequence shows diffuse moderate enhancement of the mass. The pituitary gland and stalk are displaced contralaterally (white arrow)

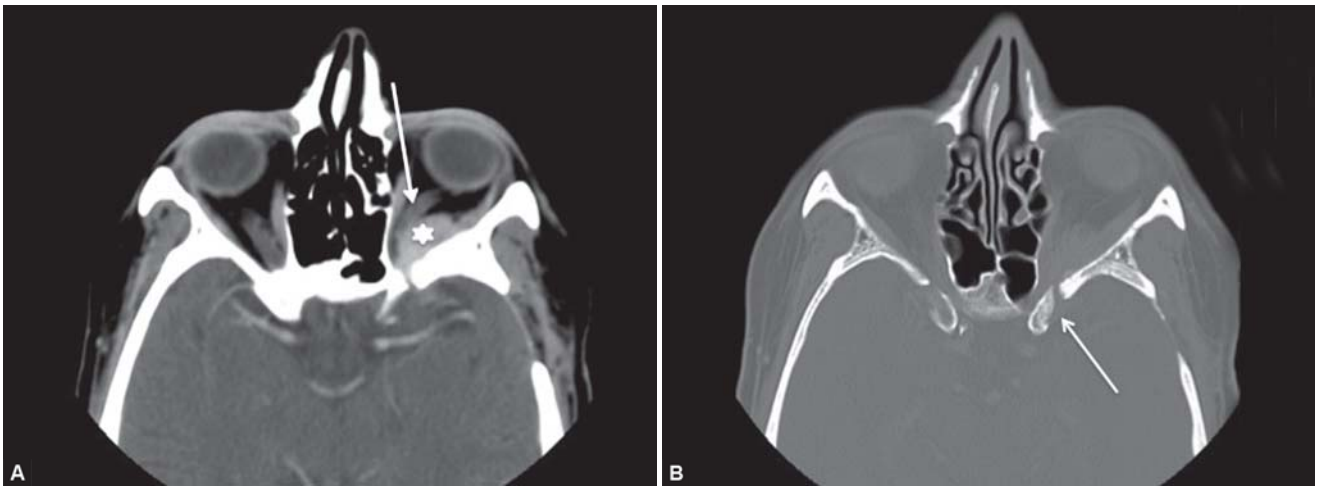

Figs 8A and B: Left orbital meningioma: (A) Axial postcontrast CT shows an ovoid enhancing intraorbital mass (*) indenting and displacing the left optic nerve (white arrow), (B) CT bone window shows hyperostosis of the adjacent left anterior clinoid process and lesser wing of sphenoid (white arrow)

NERVE SHEATH TUMORS

They comprise of schwannomas and neurofibromas, which can affect any cranial nerve, commonest in the parasellar region being a trigeminal nerve schwannoma. Involvement of the 3rd, 4th, and 6th nerves is rare.[23,33-35] The parasagittal central skull base, CP angle and the jugular foramen are common sites of involvement. Sinonasal schwannomas are rare and possibly arise from the olfactory nerve or a meningeal branch of the trigeminal nerve.[11] They appear hypointense on T1-weighted images, intermediate to hyperintense on T2-weighted images and reveal moderate contrast enhancement. On CT they are seen as well-defined tumors, which can cause smooth scalloping of the adjacent bone.

PITUITARY ADENOMA

Pituitary macroadenomas are tumors involving the sellar-suprasellar region in adults. They are usually solid, cellular tumors, with areas of necrosis and hemorrhage occurring in larger lesions. Widening of the sellar floor can be seen. When there is a suprasellar component a 'Figure of 8' appearance is seen due to indentation at the diaphragmatic sella (Figs 9A and B). These tumors displace the optic chiasm superiorly. Laterally they can extend into the cavernous sinus, which signifies poor prognosis. Invasive adenomas can involve the sellar floor with extension into the sphenoid sinus and the clivus[25-27,29] (Figs 11A and B). Erosion of the sellar floor can causes CSF leaks through the sphenoid bone.[22,33]

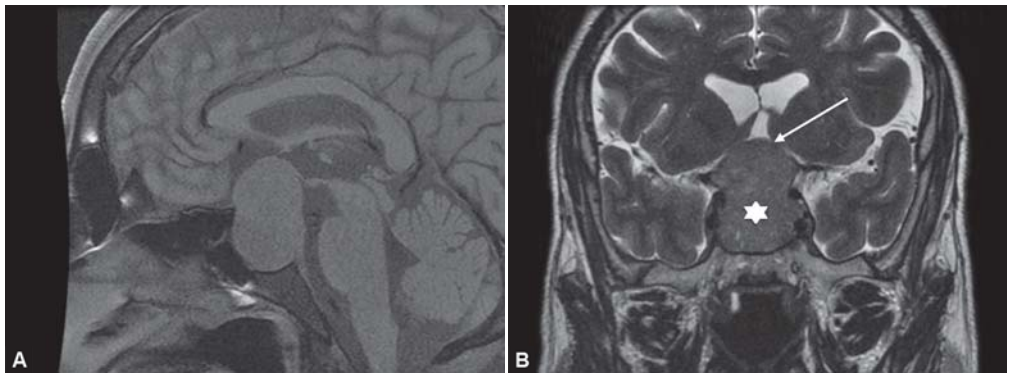

Figs 9A and B: Pituitary adenoma in a 45-year-old male: (A) Sagittal precontrast fat saturated T1-weighted sequence of the brain showing a large lobulated hypointense sellar–suprasellar mass lesion, causing widening of the sellar floor, (B) coronal T2-weighted sequence shows an isointense sellar-suprasellar mass. (*) The optic chiasm is stretched out and displaced superiorly (white arrow)

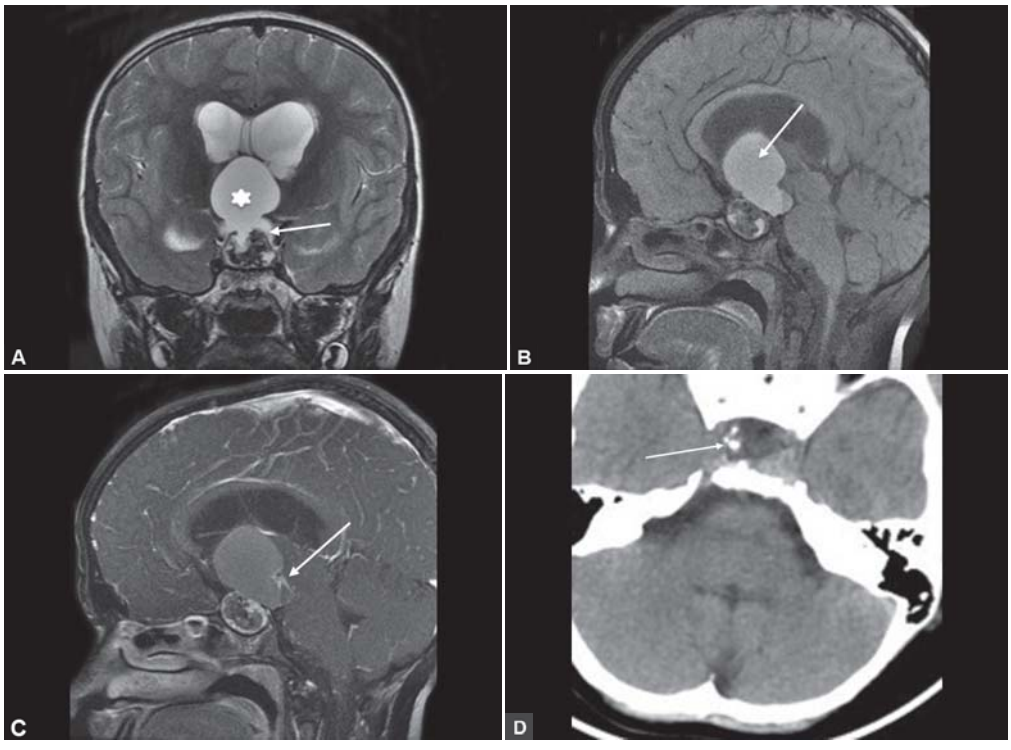

Figs 10A to D: Craniopharyngioma in an 18-year-old female: (A) Coronal T2-weighted sequence shows a solid cystic sellar—suprasellar mass (*) with hypointense calcific foci within (white arrow), (B) sagittal precontrast fat saturated T1-weighted sequence reveals T1 hyperintensity cystic contents (white arrow), (C) sagittal postcontrast fat saturated T1-weighted sequence reveals peripheral enhancement (white arrow), (D) axial plain CT scan of the brain reveals nodular calcific areas in the sella on the right side (white arrow)

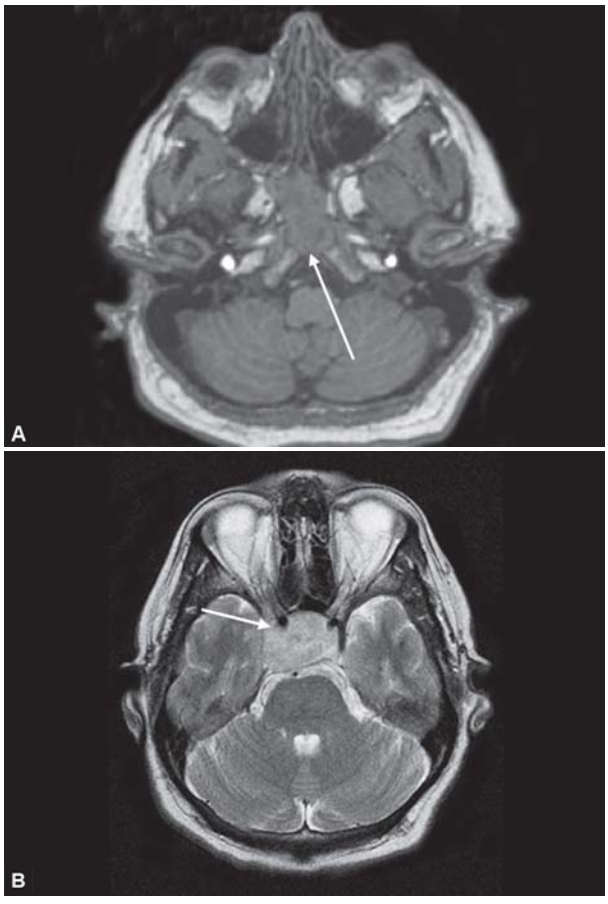

Figs 11A and B: Neuronavigation study done in a 45-year-old female with invasive pituitary adenoma. (A) Axial T1 SPGR sequence of the brain shows erosion of the clivus (white arrow) by the sellar mass, (B) axial T2-weighted sequence shows extension of the hyperintense mass lateral to the cavernous segment of the internal carotid artery suggestive of cavernous sinus invasion (white arrow)

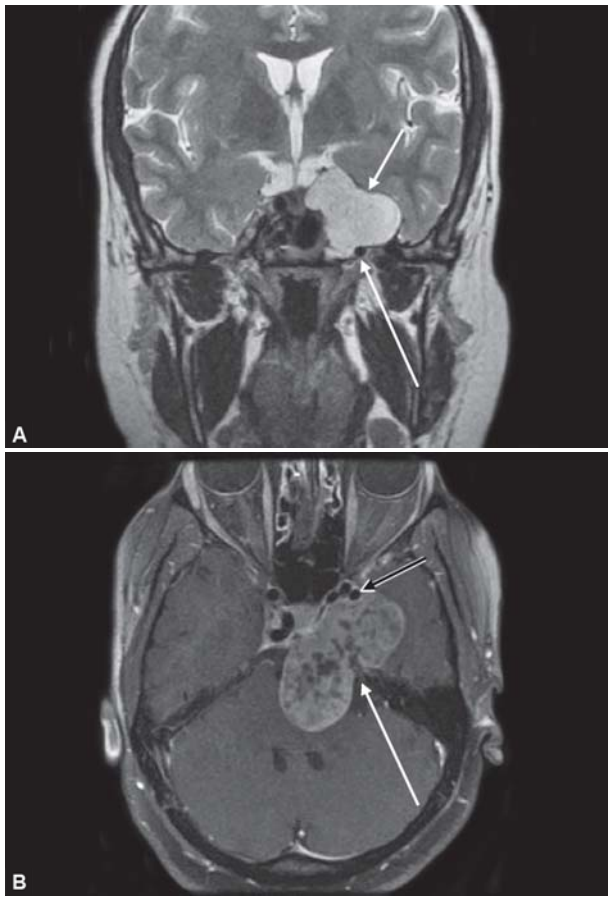

Figs 12A and B: Skull base chondrosarcoma in a 28-year-old female, who presented with left 6th nerve palsy: (A) Coronal T2-weighted image shows a large lobulated hyperintense mass lesion in the left cavernous sinus and medial temporal region (arrows); (B) axial postcontrast fat suppressed T1-weighted sequence shows heterogeneous enhancement within this lesion (white arrow), with extension into prepontine cistern and anteroinferior displacement of left cavernous ICA (black arrow)

CRANIOPHARYNGIOMA

Three percent of all intracranial neoplasms are craniopharyngiomas.[22,34] They are benign tumors and arise from the squamous epithelial remnants of the involuted hypophyseal pars tuberalis.[22,23,36,37] They have a bimodal peak of incidence in the 2nd and 6th decade. Most commonly they are suprasellar in location. Imaging findings are characteristic and are seen as large suprasellar masses with cystic areas and calcification within.[25-27,30,38] Marked enhancement of the solid component is seen on the postcontrast images. The cystic component can be hyperdense on the T1-weighted images owing to the presence of high protein concentration, cholesterol and methemoglobin.[39,40] On T2-weighted images the cystic component appears hyperintense. Calcification is better appreciated on CT (Figs 10A to D). Surgical resection is the treatment of choice.

SARCOMA

Chondrosarcomas in adults and rhabdomyosarcomas in the pediatric population are the common sarcomas in the head and neck region. Primary Ewings sarcoma rarely occurs in the head and neck region. If seen then it should be considered as a metastatic lesion from an infraclavicular primary.[11]

Chondrosarcomas are common tumors of the skull base region and arise from the cartilaganeous elements in the petro-occipital fissure. Basisphenoid and junction of the vomer with the sphenoid and ethmoid sinuses are other sites of involvement.[1] Skull base chondrosarcomas are low grade lesions and usually present with 6th nerve palsy. CT is useful in depicting the bony destruction and ring and arc matrix calcification, which are classical features of these tumors. On MRI, they appears markedly hyperintense on T2-weighted images which is very typical of chondroid lesions (Figs 12A and B). MR also helps in the relation of the tumors with the adjacent neurovascular structures. Enhancement of the soft tissue component is seen on postcontrast images, which is mostly heterogeneous. Clival chordoma is a differential in this location, however, they do not have the characteristic calcification of chondrosarcomas and are usually midline in location, whereas chondrosarcomas are more lateral in location.

Rhabdomyosarcomas can be seen in the sinonasal region, infratemporal fossa and nasopharynx. They are large fleshy tumors which appear isointense on T1-weighted, moderately hyperintense on T2-weighted images and reveal intense postcontrast enhancement. Bone destruction is also often seen.

CHORDOMA

Base skull chordoma is classically seen as a midline clival mass lesion. It arises from the notochordal rest cells that are entrapped within the basisphenoid.[25,31,32,41,42] Other rarer sites include the nasopharynx or the intracranial compartment.[25,41] They usually present with headaches, visual disturbances and various cranial nerve palsies depending on the extent of involvement. Complete surgical resection in difficult due to their close proximity to critical neurovascular structures. On CT, bony destruction of the clivus is seen. Large areas of calcification within are frequently noted. Owing to the presence of areas of hemorrhage, cystic changes and mucoid material within the MR appearance is variable.

METASTASES

Skull base is a common site for osseous metastases from a breast, lung and renal primary. Imaging reveals bony erosion/destruction and focal replacement of the marrow by a soft tissue mass. Osseous involvement is better appreciated on CT. On MR, they are usually appear as hypointense lesions replacing the normal fatty marrow on precontrast T1-weighted images. Prior knowledge of a known primary is important for the diagnosis.

INVASIVE FUNGAL SINUSITIS

Acute invasive fungal sinusitis is a rapidly progressive infection, which occurs in immunocompromised patients and in patients with uncontrolled diabetes. It has a very fulminant course with rapid intracranial and intraorbital involvement, which warrants prompt aggressive surgical debridement and systemic antifungal therapy. The reported mortality is very high, ranging from 50 to 80%.[43] Patients commonly present with fever, facial and periorbital pain and swelling, nasal congestion, rhinorrhea, and headache. Sometimes they present with blurring of vision or ophthalmoplegia. 80% of the patients with uncontrolled diabetes are affected by the fungi in order of zygomycetes, whereas 80% of the immunocompromised patients are affected by the aspergillus species.[44] It affects the mucosa and submucosa of the sinonasal region with spread along the blood vessels and bony walls. On CT, initially it is seen as hypodense mucosal thickening or soft tissue is seen within the nasal cavity and the sinus, which is usually unilateral. Fat stranding and soft tissue when seen in the

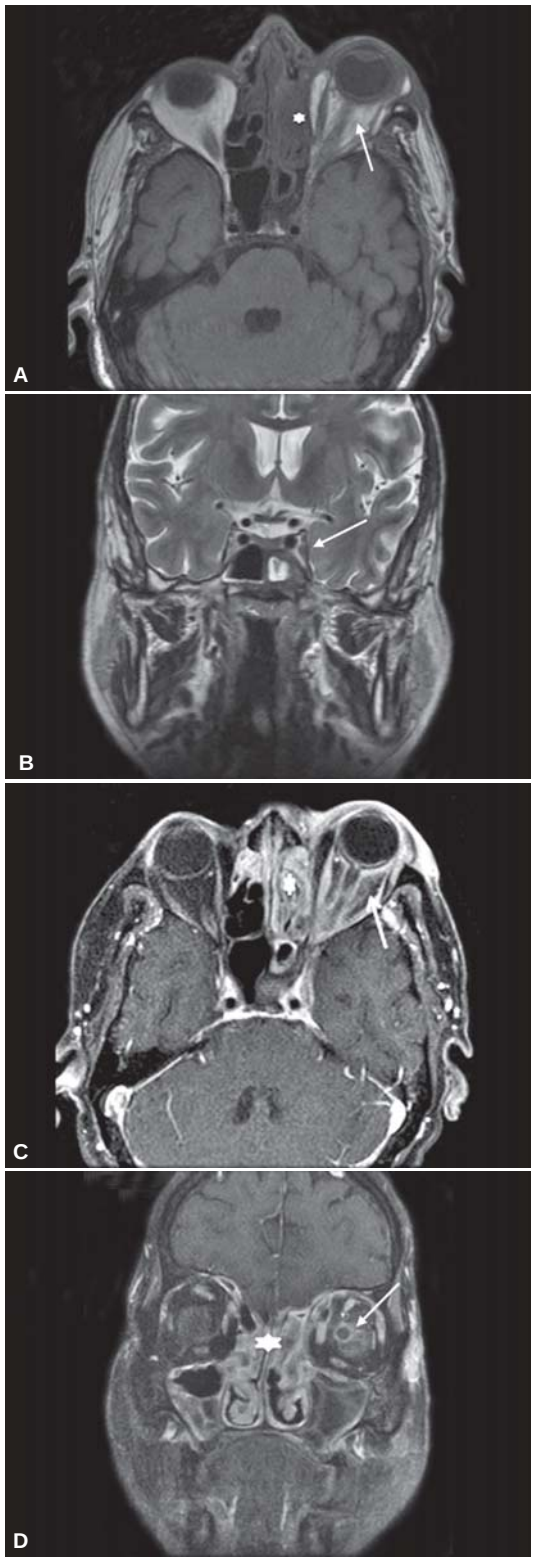

Figs 13A to D: Invasive fungal sinusitis in a 57-year-old male: (A) Axial T1-weighted precontrast sequence shows left orbital proptosis with retroocular fat stranding (white arrows) and opacification of the left ethmoid air cells (*), (B) coronal T2-weighted sequence reveals thickening of the nerves within the left cavernous sinus (white arrow), suggesting perineural spread. (C) Axial T1-weighted fat saturated postcontrast sequence reveals smudgy enhancement in the left retroocular fat, optic nerve sheath, posterior to the globe (white arrows) and left ethmoid air cells (*) with asymmetrical enhancement of the left cavernous sinus, (D) coronal postcontrast T1-weighted fat saturated sequence reveals enhancement of the left optic nerve sheath and retroocular fat (white arrow) with enhancement of bilateral ethmoid air cells (*)

retroantral fat plane and anterior periantral region represent early signs of invasiveness and should always be looked for.[45] Bone erosion and destruction are better visualized on CT. Perivascular spread, beyond the sinus can occur around the penetrating blood vessels without involving the bone. Intraorbital and intracranial involvement is better evaluated on MR. Imaging features of orbital invasion are inflammatory changes in the orbital fat and extraocular muscles and proptosis (Figs 13A to D). Due to its angiocentric nature the infection can involve the cavernous sinus and the internal carotid artery. Vascular thrombosis leads to parenchymal hemorrhage and infarcts. Similar to periantral soft tissue, for intracranial invasion, leptomeningeal enhancement is an early sign. Epidural and cerebral abscesses are late presentations. In the appropriate clinical setting, a low threshold of suspicion is necessary to make the diagnosis of invasive fungal sinusitis, both radiologically and clinically.

MUCOCELE

Mucoceles are benign expansile lesions of the sinuses which occur secondary to osteal obstruction. The most common causes of mucoceles are chronic infection, allergic sinonasal disease, trauma and previous surgery. They consist of mucoid secrections which are lined by epithelium. Frontal sinus is the commonest site (65%), followed by the ethmoid sinus (25%). Maxillary and sphenoid sinuses mucoceles are rare (<10%).[9] On CT they appear as hypodense lesions which fill the sinus and expand it. Bone attenuation with erosions can be seen due to the presence effect. However, unlike carcinomas, frank destruction is not seen. MR imaging is usually not required. The appearance on MR depends on the protein content of the lesion. Commonly seen patterns are moderate to marked T1 and T2 hyperintensity and moderate to marked T1and T2 hypointensity. Postcontrast T1-weighted images reveal linear peripheral enhancement as against carcinomas which have central enhancement as well.

INFLAMMATORY PSEUDOTUMOR

It is a rare benign lesion, of unknown etiology, also known as inflammatory myofibroblastic tumor. One of the commonest site in the head and neck region is the orbit. The nasal cavity, the nasopharynx and the maxillary sinuses are other sites of occurrence.[46] They usually present with local pain and swelling with associated constitutional symptoms, such as fever, weight loss and malaise. Pseudotumors involving the sinonasal region are seen as large masses, which appear more aggressive than those of the orbit. Commonly seen is associated bony erosion, remodeling, and sclerosis.[47,48] A characteristic finding on MR is low signal on T2-weighted images (Figs 14A to D). Homogeneous enhancement is seen on postcontrast images.

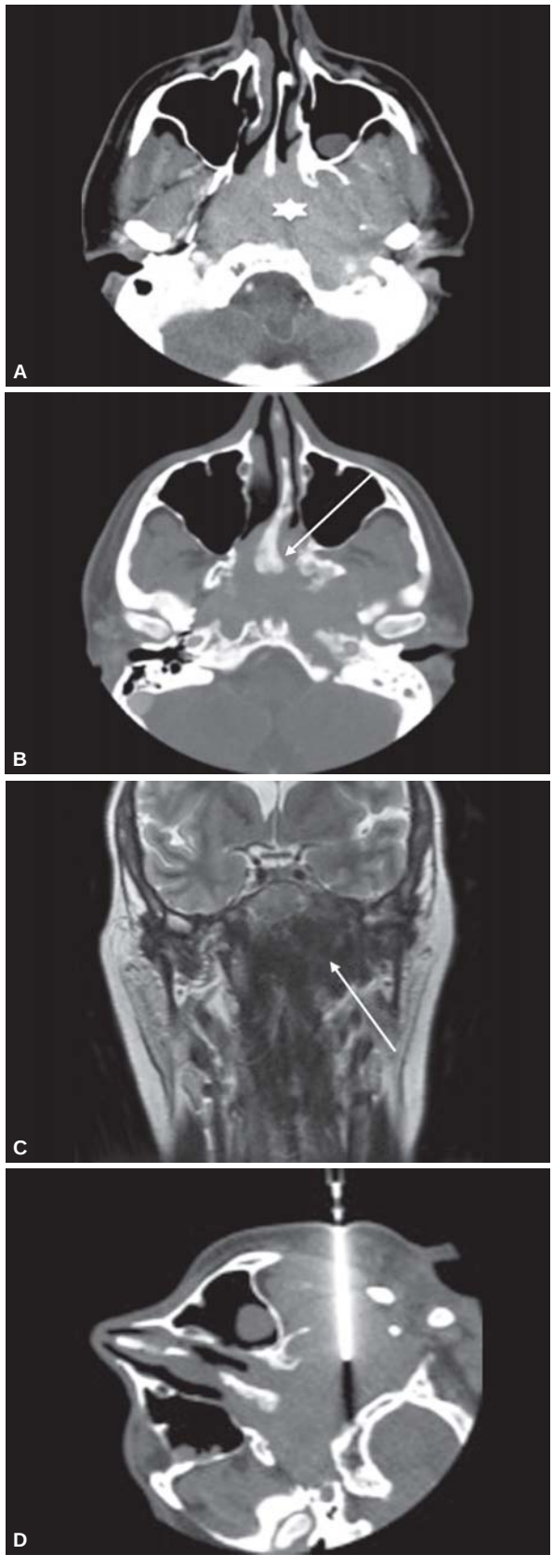

Figs 14A to D: Skull base pseudotumor in a 28-year-old male: (A) Axial postcontrast CT shows a large enhancing mass lesion (*) involving the nasopharynx, masticator space medially and the skull base, (B) CT bone window shows patchy hyperostosis and erosions of the left pterygoid plates, petroclival region and posterior aspect of the nasal septum (white arrow), (C) coronal T2-weighted sequence shows the mass to be markedly hypointense (*), (D) CT guided biopsy image with the needle *in situ*

As these lesions mimic malignancy, familiarity of the radiologist with this condition is necessary as it can prevent radical surgery. Image-guided biopsies can also be performed. Pathology reveals spindle cells interspersed with variable amounts of extracellular collagen, plasma cells and lymphocytes.[47,49,50]

SKULL BASE INFECTIONS

Diabetics and immunocompromised patients are more prone to get affected, especially in fungal infections. The disease can progress from osteomyelitis to intracranial extension in the form of meningitis, subdural empyema and abscess. Tuberculous skull base osteomyelitis is usually due to direct extension of otomastoiditis or sinonasal tuberculosis and rarely from meningitis.[51,52] Bone erosions and destruction are seen on CT; however, MRI is more useful to look for early marrow involvement, intracranial extension and abscess formation (Figs 15 and 16). As the imaging findings are nonspecific, histopathological confirmation and culture sensitivity is required which can be performed under CT guidance.

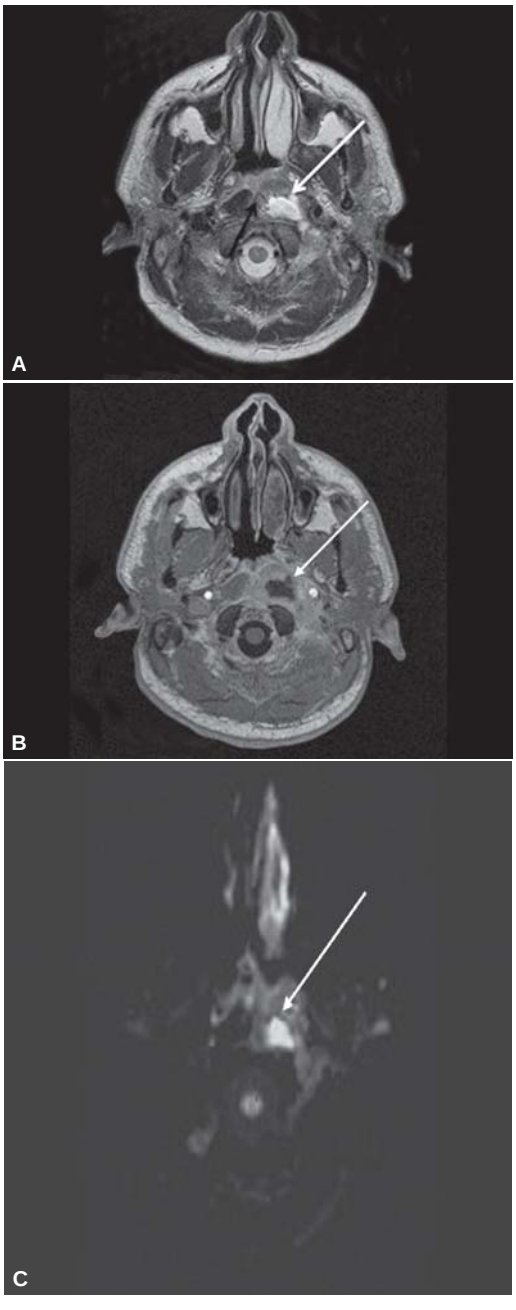

Figs 15A to C: Prevertebral abscess in a 26-year-old male. (A) Axial T2-weighted sequence shows a focal hyperintense lesion in the prevertebral region (white arrow) with diffuse edema in the right prevertebral muscles, (B) axial T1-weighted fat saturated postcontrast sequence shows peripheral enhancement with central necrosis (white arrow), (C) diffusion weighted sequence shows restricted diffusion in the abscess (white arrow)

CSF FISTULA

CSF fistula refers to leak of CSF from the intracranial space through a bony defect in the skull base. CSF leaks are classified into traumatic, nontraumatic and spontaneous.[53] Traumatic account for almost 90% of cases. Majority (80%) of these present as rhinorrhea (leak through the nose) and the others (20%) present as otorrhea (leak through the ear).[53] Traumatic leaks include post traumatic fractures of the anterior cranial fossa, central skull base and lateral skull fractures. Postoperative leaks are also included in this category. Nontraumatic include the congenital lesions, tumors and increased intracranial pressure conditions. The

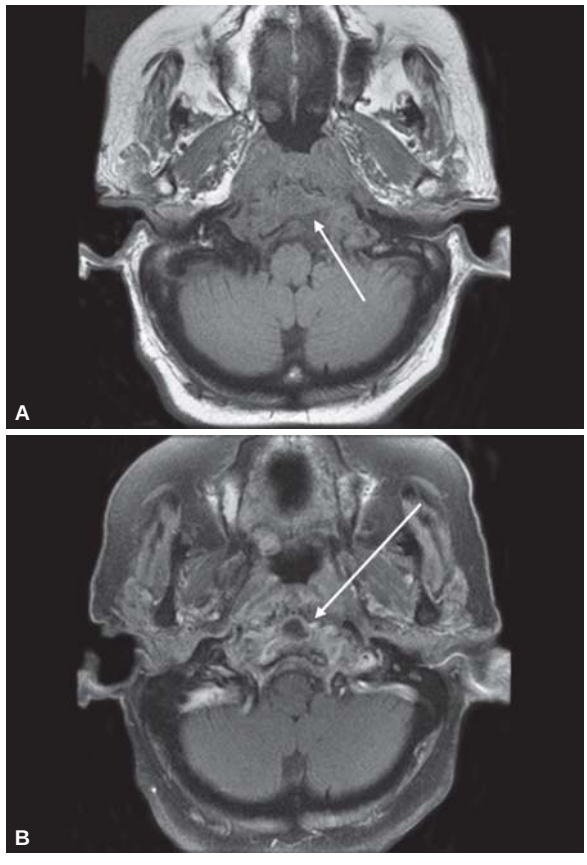

Figs 16A and B: Skull base osteomyelitis in a 57-year-old diabetic female: (A) Axial T1-weighted sequence shows loss of the normal hyperintense marrow signal with ill-defined hypointensity in the clivus (white arrow), (B) axial T1-weighted fat saturated postcontrast sequence reveals heterogeneous enhancement of the clivus and surrounding soft tissues (white arrow)

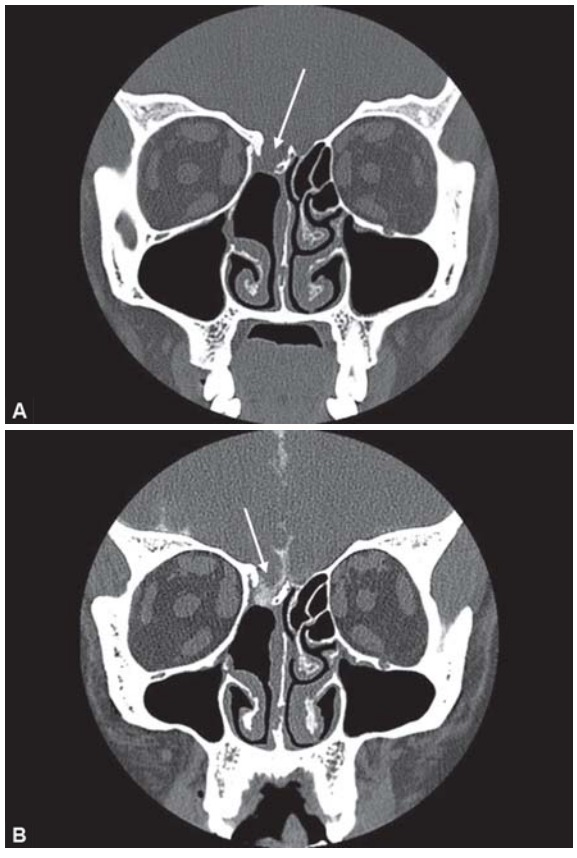

Figs 17A and B: CT cisternography in a 40-year female, with recurrent right nasal leak, following prior repair of CSF leak: (A) Plain coronal CT shows a large defect in the roof of right ethmoid/cribriform (arrow), with right-sided postoperative nasal bony defects, (B) postcisternography coronal CT shows extension of the intrathecally administered subarachnoid contrast across this site (arrow), confirming the site of recurrent leak

spontaneous CSF fistula is commonly seen in obese middle aged women in whom no other cause of CSF leak is found.[53] CSF leaks have a high risk of ascending meningitis estimated to be about 30 to 40%.[54,55] Minimally invasive intranasal endoscopic repair treats more than 90% of CSF leaks.[54-56] Preoperative imaging is imperative to confirm and delineate the exact site of leak, to find the cause in case of non-traumatic leaks and to look for any associated encephalocele/meningocele. Modalities available are plain and CT cisternography, MRI and radionuclide cisternography. At our institute we do a plain high resolution 0.6 mm coronal MDCT using a bone algorithm. Presence of a bony defect is looked for. A CT cisternography is performed to confirm the leak of contrast (Figs 17A and B), across the suspected site on plain CT and in case of multiple bony defects to pinpoint the exact site of leak, as not all defects leak. Contraindications include meningitis and raised intracranial tension. A lumbar puncture is performed and approximately 10 ml of 300 mg/ml of nonionic contrast is injected. Cotton pledgets are put in both nostrils and ears. Patient is then placed in head low position and decubitus positions for approximately 45 min following which a repeat coronal CT scan is performed. Increased CT attenuation on either side of the bony defect is looked for and these findings are corroborated with the plain scan. The exact site and size and distance from important bony landmarks, e.g. orbitocranial canal is included in the report. Pledgets are also scanned separately to look for their opacification with high density contrast. Sensitivity of CT cisternography to detect active CSF leaks is 92%, but is only 40% when the leak is intermittent.[57] MR is a noninvasive technique for identifying CSF leaks. Typically multiplanar, thin heavily T2-weighted sequences and FIESTA are obtained. CSF leaks are identified as continuity of the CSF through the subarachnoid space into the adjacent sinus. MR has a sensitivity of 85% in locating CSF leaks. Limitation of MR is in depicting the fine bony detail which is useful in planning surgery and at times difficulty in differentiating inflammatory sinus soft tissue from CSF, especially when the defect is tiny and patient is not leaking at the time of imaging. Common sites for CSF leaks are cribriform plate, anterior and posterior ethmoid, sphenoid and frontal sinuses. Less commonly CSF leaks occur through the tegmen tympani. It is important to always evaluate the temporal bone structures for CSF leaks, in all cases.

Radionuclide cisternography is used when CT does not show a defect and beta-2 transferrin cannot be collected, and there is high index of suspicion for CSF leak.

CONGENITAL NASOFRONTAL MASSES

They usually present at birth and occur due to an abnormal regression of the embryologic dural diverticulum from the prenasal space. They are intranasal when the dura mater extends through the foramen cecum into the prenasal space and nasal cavity and extranasal when the dural diverticulum herniates through the foramen cecum and fonticulus frontalis (embryologic gap between the nasal and frontal bones which later fuses to form frontonasal suture) Common congenital anomalies involving the nasofrontal region are encephaloceles, nasal gliomas, dermoid and epidermoids.[58-60] Preoperative imaging is useful for identifying their location and classifying them as intra/extranasal or combination of both as the surgical approach varies accordingly. High resolution CT is useful in defining the skull base anatomy prior to surgery. MRI is very useful for delineating the defects and the herniated contents or mass lesion. Of special importance in these cases are the sagittal thin T2-weighted and FIESTA sequences.

Encephaloceles are uncommon congenital lesions arising due to herniation of the intracranial contents into the extracranial space. They are associated with other facial anomalies, endocrine dysfunction and mental retardation. Associated risk of CSF rhinorrhea and meningitis is also known. They are classified according to their location, details of which are beyond the scope of this article. Common

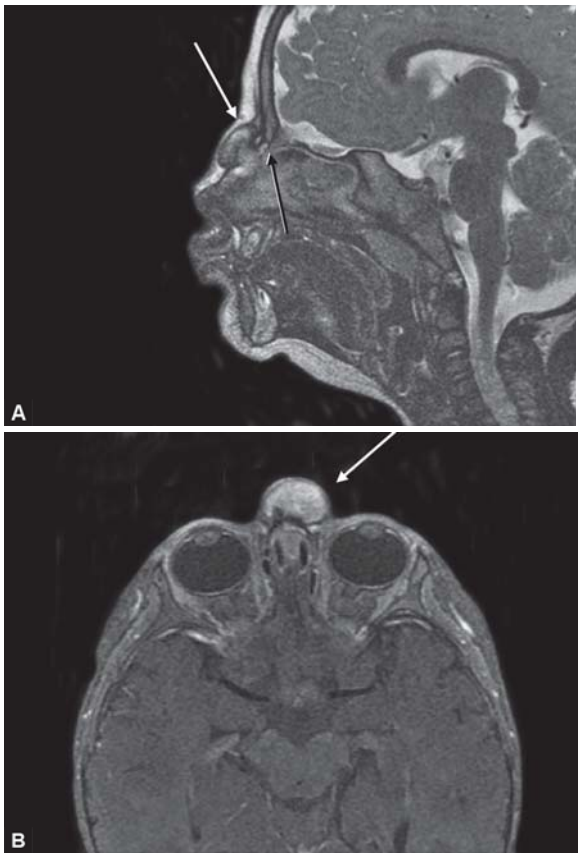

Figs 18A and B: Nasal glioma in a 1-year-old male child: (A) Sagittal T2-weighted sequence shows a focal mass lesion in the prenasal space (white arrow) continuous with a linear tract which extends up to the foramen caecum (black arrow), (B) axial T1-weighted fat saturated postcontrast sequence shows diffuse enhancement of the mass (white arrow)

ones are the frontonasal and nasoethmoidal. The former are extranasal glabellar masses, while the latter are located in the prenasal space and nasal cavity. Meningoceles follow CSF density on all sequences and are seen as outpouchings which are continuous with the intracranial CSF. Meningoencephaloceles are isointense to the cerebral cortex on all sequences. In case of associated dysplasia and gliosis, they can appear hyperintense on T2-weighted images.

Gliomas result from sequestered neurogenic tissue in the extracranial region due to faulty regression of the dural diverticulum. They can be extranasal (60%) intranasal (30%), or a combination of both (10%).[58,61,62] They are not true gliomas as they do not contain any neoplastic tissue. The intranasal type are attached to the superolateral nasal wall, nasal turbinate or less often to the nasal septum and are sequestered between the nasal bony and nasal capsule. Extranasal on the other hand are skin covered and are seen at the glabella. On MRI, they are hypointense to cortex on T1-weighted sequences and hyperintense on T2 and PD sequences (Figs 18A and B).

Occasionally skin elements can get trapped within the prenasal space when the dural diverticulum regresses, giving rise to formation of dermoid and epidermoids. A mass or a sinus tract is seen, along the path of regression of the dural diverticulum anywhere from the columella to anterior cranial fossa.[58,59,63] Associated skin dimpling, tuft of hair or sinus tract can be seen. Dermoid cysts contain ectoderm with skin appendages, unlike epidermoid which contain only ectodermal elements. Dermoids are midline lesions and are commonly seen at the glabella. Epidermoids on the other hand are paramidline in location and occur near the collumella.[58,59,61,64] MR is the imaging modality of choice and helps in identifying intracranial extension. Dermoids are hyperintense on T1 and T2-weighted images while epidermoids usually follow CSF intensity and are hypointense on T1-weighted images and hyperintense on T2-weighted images. A classical feature of epidermoids is that they reveal restricted diffusion. This feature not only helps in the diagnosis but is also useful to look for postoperative residual/recurrent disease.

CONCLUSION

Imaging is an important tool to study the anterior skull base, due to its complex anatomy. MRI and CT are primary imaging modalities to image the skull base and these should be judiciously used to complement each other, in order to provide detailed anatomical landmarks as well as morphological characterization, so as to guide the surgeon and for further management, as we have briefly discussed in this article.

REFERENCES

1. Durden DD, Williams DW 3rd. Radiology of skull base neoplasms. Otolarygngol Clinics North Am 2001;34:1043-64.
2. Connors JJ, Wojak JC. Juvenile nasopharyngeal angiofibromas, international neuroradiology: Strategies and practical techniques. Philadelphia:WB Saunders 1999:121-30.
3. Ludwig BJ, Foster BR, Saito N, Nadgir RN, Castro-Ragon I, Sakai O. Diagnostic imaging in nontraumatic pediatric head and neck emergencies. Radiographics 2010;30(3):781-99.
4. Laine FJ, Nadel L, Braun IF. CT and MR imaging of the central skull base. Part 2. Pathologic spectrum. Radiographics 1990;10(5):797-821.
5. Chong VF, Khoo JB, Fan YF. Fibrous dysplasia involving the base of the skull. AJR Am J Roentgenol Mar 2002;178(3): 717-20.
6. Brown EW, Megerian CA, McKenna MJ, Weber A. Fibrous dysplasia of the temporal bone. Am J Roentgenol 1995; 164(3):679-82.
7. Chong VF, Khoo JB, Fan YF. Imaging of the nasopharynx and skull base. Neuroimag Clin N Am 2000;14:695-719.
8. Resnick D. Tuberous sclerosis, neurofibromatosis and fibrous dysplasia. In: Feldman D (Ed). Diagnosis of bone and joint disorders, 3rd ed. Philadelphia: Saunders 1995:4353-95.
9. Som PM, Curtin HD. Head and neck imaging, tumor and tumor-like conditions (4th ed). St Louis (MO): Mosby Year Book 2003:261-373.
10. Grossman RI, Yousem DM. Neuroradiology: The requisites. St Louis: Mosby 1994:359-76.
11. Parmar H, Gujar S, Shah G, Mukherji SK. Imaging of the anterior skull base. Neuroimaging Clin N Am 2009;19(3):427-39.
12. Som PM, Curtin HD. Lewis JS, Castro EB. Cancer of the nasal cavity and paranasal sinuses. J Laryngol Otol 1972;86:255-62.

13. Vrionis Fd, Kienstra MA, Rivera M, Padhya TA. Malignant tumors of the anterior skull base. Cancer Control 2004;11(3) 144-51.
14. Ginsberg LE. MR imaging of perineural tumor spread. Neuroimaging Clin N Am 2004;14(4):663-77.
15. Stern SJ, Hanna E. Cancer of the nasal cavity and paranasal sinuses. In: Myers EN, Suen JY (Eds). Cancer of the head and neck (3rd ed). Philadelphia: WB Saunders Co 1996;205-33.
16. Hurst RW, Erickson S, Cail WS, Newman SA, Levine PA, Burke J, et al. Computed tomographic features of esthesioneuroblastoma. Neuroradiology 1989;31(3):253-57.
17. Connor SE, Umaria N, Chavda SV. Imaging of giant tumours involving the anterior skull base. Br J Radiol Jul 2001; 74(883):662-67.
18. Som PM, Lidov M, Brandwein M, et al. Sinonasal-esthesioneuroblastoma with intracranial extension: Marginal tumor cysts as a diagnostic MR finding. Am J Neuroradiol 1994;15:1259-62.
19. Barnes L, Verbin RS, Gnepp DR. Diseases of the nose, paranasal sinuses and nasopharynx. In: Barnes L (Ed). Surgical pathology of the head and neck. New York: Marcel Decker; 1985;1: 403-51.
20. Barnes EL, Kapadia SB, Nemzek WR, et al. Biology of selected skull base tumors. In: Janecka IP, Tiedmann K (Eds). Skull base surgery. Philadelphia: Lippincott-Raven 1997;263-92.
21. Som PM, Dillon WP, Sze G, Lidov M, Biller HF, Lawson W. Benign and malignant sinonasal lesions with intracranial extension: differentiation with MR imaging. Radiology Sep 1989;172(3):763-66.
22. Felsberg GJ, Tien RD. Sellar and parasellar lesions involving the skull base. Neuroimaging Clin N Am Aug 1994;4(3):543-60.
23. Chong BW, Newton TH. Hypothalamic and pituitary pathology. Radiol Clin North Am 1993 Sep;31(5):1147-53.
24. Zimmerman RA. Imaging of intrasellar, suprasellar and parasellar tumors. Semin Roentgenol Apr 1990;25(2):174-97.
25. Alexandra B. Imaging of the central skull base. Neuroimaging Clin N Am 2009;19(3):441-68.
26. Curtin HD, Chavali R. Imaging of the skull base. Radiol Clin North Am 1998;36(5):801-17.
27. Atlas SW. Magnetic resonance imaging of the brain and spine. (3rd ed). Philadelphia: Lippincott Williams and Wilkins 2002.
28. Ehab Y, Hanna, DeMonte Franco. Comprehensive management of skull base tumors (1st ed). New York: London. Informa Healthcare 2009.
29. Borges A. Skull base tumors part II: Central skull base tumors and intrinsic tumors of the bony skull base. Eur J Radiol 2008;66:348-62.
30. Casselman JW. The skull base: Tumoral lesions. Eur Radiol 2005;15(3):534-42.
31. Lufkin R, Borges A, Villablanca P. Teaching atlas of head and neck imaging (1st ed). New York: Thieme 2000:3-31.
32. Lufkin R, Borges A, Nguyen K, et al. MRI of the head and neck. (2nd ed). MRI teaching file series. Philadelphia: Lippincott Williams 2001.
33. Chandler WF. Sellar and parasellar lesions. Clin Neurosurg 1991;37:514-27.
34. Johnsen DE, Woodruff WW, Allen IS, Cera PJ, Funkhouser GR, Coleman LL. MR imaging of the sellar and juxtasellar regions. Radiographics. Sep 1991;11(5):727-58.
35. Yasui T, Hakuba A, Kim SH, Nishimura S. Trigeminal neurinomas: Operative approach in eight cases. J Neurosurg Oct 1989;71(4):506-11.
36. Petito CK, DeGirolami U, Earle KM. Cranipharyngiomas: A clinical and pathological review. Cancer Apr 1976;37(4): 1944-52.
37. Rutka JT, Hoffman HJ, Drake JM, Humphreys RP. Suprasellar and sellar tumors in childhood and adolescence. Neurosurg Clin North Am Oct 1992;3(4):803-20.
38. Fishbein NJ, Kaplan MJ. Magnetic resonance imaging of the central skull base. Top Magn Reson Imaging 1999;10(5): 325-46.
39. Elster AD. Modern imaging of the pituitary. Radiology Apr 1993;187(1):1-14.
40. Pusey E, Kortman KE, Flannigan BD, Tsuruda J, Bradley WG. MR of craniopharyngiomas: Tumor delineation and characterization AJR Am J Roentgenol Aug 1987;149(2): 383-88.
41. Pamir MN, Ozduman K. Analysis of radiological features relative to histopathology in 42 skull base chordomas and chondrosarcomas. Eur J Radiol 2006;58(3):461-70.
42. Crockard A. Chordomas and chondrosarcomas of the cranial base: Results and follow-up of 60 patients. Neurosurgery 1996;38(2):420-27.
43. Waitzman AA, Birt BD. Fungal sinusitis. J Otolaryngol 1994;23(4):244-49.
44. Aribandi M, McCoy VA, Bazan C (3rd). Radiographics Sep-Oct 2007;27(5):1283-96.
45. Silverman CS, Mancuso AA. Periantral soft-tissue infiltration and its relevance to the early detection of invasive fungal sinusitis: CT and MR findings. Am J Neuroradiol Feb 1998;19(2):321-25.
46. Som PM, Brandwein MS, Maldjian C, Reino AJ, Lawson W. Inflammatory pseudotumor of the maxillary sinus: CT and MR findings in six cases. Am J Roentgenol 1994;163:689-92.
47. Park SB, Lee JH, Weon YC. Imagingfindings of head and neck inflammatory pseudotumor. Am J Roentgenol Oct 2009; 193(4):1180-86.
48. De Vuysere S, Hermans R, Sciot R, Crevits I, Marchal G. Extraorbital inflammatory pseudotumor of the head and neck: CT and MR findings in three patients. Am J Neuroradiol 1999;20:1133-39.
49. Narla LD, Newman B, Spottswood SS, Narla S, Kolli R. Inflammatory pseudotumor. Radio Graphics 2003;23:719-29.
50. Park SB, Cho KS, Kim JK, et al. Inflammatory pseudotumor (myoblastic tumor) of the genitourinary tract. Am J Roentgenol 2008;191:1255-62.
51. Sencer S, Sencer A, Aydin K, Hepgül K, Poyanli A, Minareci O. Imaging in tuberculosis of the skull and skull-base: Casereport. Neuroradiology Mar 2003;45(3):160-63.
52. Gupta RK, Jena A, Sharma A. Sellar abscess associated with tuberculous osteomyelitis of the skull: MR findings. Am J Neuroradiol 1989;10(2):448.
53. Lloyd KM, DelGaudio JM, Hudgins PA. Imaging of skull base cerebrospinal fluid leaks in adults. Radiology Sep 2008;248(3):725-36.
54. La Fata V, McLean N, Wise SK, DelGaudio JM, Hudgins PA. CSF leaks: Correlation of high-resolution CT and multiplanar reformations with intraoperative endoscopic findings. Am J Neuroradiol Mar 2008;29(3):536-41.
55. Schlosser RJ, Bolger WE. Nasal cerebrospinal fluid leaks: Critical review and surgical considerations. Laryngoscope 2004;114: 255-65.
56. McMains KC, Gross CW, Kountakis SE. Endoscopic management of cerebro-spinal fluid rhinorrhea. Laryngoscope 2004;114:1833-37.
57. Shetty PG, Shroff MM, Sahani DV, et al. Evaluation of high-resolution CT and MR cisternography in the diagnosis of cerebrospinal fluid fistula. Am J Neuroradiol 1998;19: 633-37.

58. Lowe LH, Booth TN, Joglar JM, Rollons NK. Midface anomalies in children. Radiographics Jul-Aug 2000;20(4):907-22.
59. Sadler TW. Langman's medical embryology (5th ed). Baltimore: Md: Williams & Wilkins 1985.
60. Barkovich AJ, Vandermarch P, Edwards MSB, Cogen PH. Congenital nasal masses: CT and MR imaging features in 16 cases. Am J Neuroradiol 1991;12:105-16.
61. Castillo M. Congenital abnormalities of the nose: CT and MR findings. Am J Roentgenol 1994;162:1211-17.
62. Paoli CH, Francois M, Triglia JM, Frydman E, Polonovski JM, Narcy PH. Nasal obstruction in the neonate secondary to nasolacrimal duct cysts. Laryngoscope 1995;105:86-89.
63. Kennard CD, Rasmussen JE.Congenital midline nasal masses: Diagnosis and management. J Dermatol Surg Oncol 1990; 16:1025-36.
64. Vogelzand PJ, Babbel RW, Harnsberger HR. The nose and nasal vault. Semin Ultrasound CT MR 1991;12:592-612.